The transcription factor Deaf1 modulates *Engrailed-1* expression to regulate skin appendage

fate

Daniel Aldea<sup>1</sup>, Blerina Kokalari<sup>1</sup>, Christine Luckhart<sup>2</sup>, Adam Aharoni<sup>1</sup>, Paul R. Albert<sup>2</sup>, Yana G.

Kamberov<sup>1,3\*</sup>

1 Department of Genetics, Perelman School of Medicine, University of Pennsylvania,

Philadelphia, PA USA

2 Brain and Mind Research Institute, Ottawa Hospital Research Institute, University of Ottawa,

Ottawa ON Canada

3 Department of Dermatology, Perelman School of Medicine, University of Pennsylvania,

Philadelphia, PA USA

\* Corresponding author: yana2@pennmedicine.upenn.edu

**ORCIDs** 

Daniel Aldea: https://orcid.org/0000-0001-5101-0194

Blerina Kokalari: https://orcid.org/0000-0003-1037-6901

Christine Luckhart: https://orcid.org/0000-0003-2269-3330

Adam Aharoni: https://orcid.org/0000-0003-3224-3851

Paul R. Albert: https://orcid.org/0000-0002-1809-3554

Yana G. Kamberov: https://orcid.org/0000-0002-6239-1831

**Short title:** Deafl is a positive modulator of Engrailed-1 and sweat gland development

**Abbreviations:** inter-footpad (IFP), standard deviation (SD)

1

#### TO THE EDITOR

In humans, eccrine sweat glands are essential for heat dissipation, which relies on cooling that results from the vaporization of sweat at the skin surface (Kuno 1956). The transcription factor Engrailed-1 (En1) is pivotal in the formation of eccrine glands (Kamberov et al. 2015; Loomis et al. 1996; Lu et al. 2016). *En1* expression is a hallmark of basal keratinocytes of eccrine gland-forming skin, and focal upregulation of *En1* is a signature of eccrine gland placodes (Kamberov et al. 2015; Lu et al. 2016). In mice, modulation of *En1* levels is an intrinsic mechanism to regulate the abundance of eccrine glands, and a modest decrease in *En1* expression is sufficient to shift the balance of appendages in the volar skin, to which eccrine glands are restricted in mice, from an eccrine to a hair follicle fate (Kamberov et al. 2015). Despite the importance of ectodermal *En1* expression in the development of eccrine glands, the molecular mechanisms controlling *En1* in this context are poorly understood.

To investigate *En1* regulation in the skin, we sought to identify transcription factors that control expression of the *En1* locus. We scanned the genomic region upstream of the *En1* open reading frame for the presence of transcription factor binding sites that are conserved among placental mammals. We identified two highly conserved DNA motifs predicted to bind the transcription factor Deaf1 (in mice, mm10, chr1 120602231bp-120602255bp; chr1 120602322bp-120602346bp; in humans, hg19, chr2 119605410bp-119605434bp; chr2 119605501-119605525bp) (Figure 1a). We performed DEAF1 ChIP-seq using an antibody against endogenous DEAF1 from a human keratinocyte cell line, GMA24F1A, which was previously shown to express *EN1* (Czesak et al. 2012; Mainguy et al. 1999) (Figure S1). We observed a peak of DEAF1 enrichment overlapping the two predicted DEAF1 binding sites (hg19 chr2 119605273bp-119605834bp), and validated this interaction by ChIP-PCR (Figure 1a, b).

To investigate whether DEAF1 can regulate the expression of *EN1*, we evaluated *EN1* levels under *DEAF1* siRNA knock-down in human keratinocytes (Figure 1c). *DEAF1* knock-down resulted in decreased *EN1* compared to control conditions (Figure 1c) indicating that DEAF1 regulates *EN1* cell-autonomously. Conversely, overexpression of DEAF1 in human keratinocytes led to a mild but significant increase in *EN1* expression (Figure 1d).

To determine if Deaf1 regulates En1 expression in the skin, we evaluated the relative expression of En1 in Deaf1 constitutive knock-out mice (Hahm et al. 2004; Luckhart et al. 2016). En1 expression was analyzed in the volar hind-limb skin on post-natal day 2, the time of ectodermal appendage specification in this region (Kamberov et al. 2015). The relative levels of En1 at this stage are critical for determining the appendage composition of the inter-footpad space (IFP), the medial volar hind-limb in which hair and eccrine glands are interspersed (Kamberov et al. 2015). Loss of Deaf1 led to a dose-dependent decrease in En1 expression, indicating that Deaf1 impacts En1 transcription during this critical developmental window (Figure 1e). In contrast, we did not detect a significant reduction in En1 expression from embryonic mouse limb buds, in which En1 is critical for maintaining ventral identity (data not shown) (Loomis et al. 1996). These and all subsequent mouse experiments were carried out in accordance with approved institutional animal protocols.

In light of the finding that *Deaf1* loss leads to reduced *En1* expression, we evaluated whether this is associated with changes in IFP ectodermal appendage composition. On average, eccrine gland number in *Deaf1* knock-out homozygotes was three fold lower than in wildtype littermates, while hair follicle number was significantly higher (Figure 2a, b, c). *Deaf1* knock-out heterozygotes exhibited an intermediate phenotype (Figure 3). Eccrine gland number was

unaffected in the foot-pads, hairless elevations that surround the IFP and have the highest level of *En1* expression of any volar skin (Figure S2).

To determine if Deaf1 effects on eccrine gland number were cell-autonomous *in vivo*, we mated mice expressing a conditional allele of Deaf1 ( $Deaf1^{I/I/I}$ ), in which loxP sites flank Deaf1 exons 2-5, to En1Cre ( $En1^{Cki}$ ) mice that harbor a knock-in of Cre recombinase into the En1 locus that also abolishes endogenous gene function (Kimmel et al. 2000; Vulto-van Silfhout et al. 2014). Consistent with our previous findings, En1Cre heterozygotes exhibited decreased IFP eccrine gland number (Kamberov et al. 2015) (Figure 2d). While our analysis was underpowered to detect changes in IFP hair follicle number, eccrine gland number in En1Cre/+;  $Deaf1^{I/I/I}$  animals was on average three fold lower than in control littermates, similar to the magnitude of change observed in the constitutive Deaf1 knock-out (Figure 2c, S3). En1Cre/+;  $Deaf1^{I/I/+}$  heterozygous mutant animals exhibited an intermediate phenotype (Figure 2c). Since En1 expression is restricted to the basal keratinocyte layer of the distal volar limb, these data indicate that Deaf1 regulation of eccrine gland development is a consequence of the activity of this factor within keratinocytes.

In this study, we have identified a transcription factor, Deaf1, which promotes eccrine gland formation. The observations that Deaf1 is enriched at *En1* in keratinocytes, and positively regulates *En1* cell-autonomously suggest that Deaf1 effects on eccrine gland formation are mediated at least in part by direct regulation of the *En1* locus. Deaf1 effects on *En1* likely require the recruitment of context-specific co-factors since Deaf1 does not contain an intrinsic transcriptional activation domain, but rather binds DNA via its SAND domain and acts as a scaffold for other proteins (Joseph et al. 2014; Michelson et al. 1999; Philippe et al. 2018). A multi-component framework, of which Deaf1 is a part, may explain why effects of *Deaf1* loss on appendage composition are more mild that those of *En1* loss (Kamberov et al. 2015; Loomis et al.

1996). Alternatively, it is possible that Deaf1 is required in some, but not all En1 expressing cells. Resolving these possibilities will require resolution of the larger molecular complex that is bound to Deaf1 and the development of genetic drivers to knock-out Deaf1 in distinct En1 expressing regions of the volar ectoderm. To our knowledge, Deaf1 is the first transcription factor implicated in the regulation of En1, a critical determinant of eccrine fate, within keratinocytes. This finding enhances understanding of the molecular mechanisms that are harnessed to drive eccrine gland specification and lays a molecular foundation for elucidating the broader En1 regulatory circuit in the skin.

#### **DATA AVAILABILITY**

The data discussed in this publication have been deposited in NCBI's Gene Expression Omnibus (Edgar et al. 2002) and are accessible through GEO Series accession number GSE129965 (https://www.ncbi.nlm.nih.gov/geo/query/acc.cgi?acc= GSE129965). All constructs used in this study are available upon request from YGK.

#### **CONFLICTS OF INTEREST**

The authors state no conflict of interest.

### **ACKNOWLEDGEMENTS**

This work was supported by a National Science Foundation grant (NSF BCS - 1847598) to YGK.

# **CRediT STATEMENT**

Conceptualization: DA, YK; Data curation: DA; Formal Analysis: DA, YK; Funding Acquisition:

YK; Investigation: DA, BK, AA; Resources: CL, PA; Visualization: DA, YK; Writing - Original

Draft Preparation: YK; Writing – Review & Editing: DA, PA, YK; Supervision: YK

# REFERENCES

Czesak M, Le François B, Millar AM, Deria M, Daigle M, Visvader JE, et al. Increased Serotonin-1A (5-HT1A) Autoreceptor Expression and Reduced Raphe Serotonin Levels in Deformed Epidermal Autoregulatory Factor-1 (Deaf-1) Gene Knock-out Mice. J. Biol. Chem. 2012;287(9):6615–27

Edgar R, Domrachev M, Lash AE. Gene Expression Omnibus: NCBI gene expression and hybridization array data repository. Nucleic Acids Res. 2002;30(1):207–10

Hahm K, Sum EYM, Fujiwara Y, Lindeman GJ, Visvader JE, Orkin SH. Defective Neural Tube Closure and Anteroposterior Patterning in Mice Lacking the LIM Protein LMO4 or Its Interacting Partner Deaf-1. Mol. Cell. Biol. 2004;24(5):2074–82

Joseph S, Kwan AH, Stokes PH, Mackay JP, Cubeddu L, Matthews JM. The Structure of an LIM-Only Protein 4 (LMO4) and Deformed Epidermal Autoregulatory Factor-1 (DEAF1) Complex Reveals a Common Mode of Binding to LMO4. PLOS ONE. 2014;9(10):e109108

Kamberov YG, Karlsson EK, Kamberova GL, Lieberman DE, Sabeti PC, Morgan BA, et al. A genetic basis of variation in eccrine sweat gland and hair follicle density. Proc. Natl. Acad. Sci. U. S. A. 2015;112(32):9932–7

Kimmel RA, Turnbull DH, Blanquet V, Wurst W, Loomis CA, Joyner AL. Two lineage boundaries coordinate vertebrate apical ectodermal ridge formation. Genes Dev. 2000;14(11):1377–89

Kuno Y. Human perspiration. Springfield, IL: Thomas; 1956.

Loomis CA, Harris E, Michaud J, Wurst W, Hanks M, Joyner AL. The mouse Engrailed-1 gene and ventral limb patterning. Nature. 1996;382(6589):360–3

Lu CP, Polak L, Keyes BE, Fuchs E. Spatiotemporal antagonism in mesenchymal-epithelial signaling in sweat versus hair fate decision. Science. 2016;354(6319):aah6102

Luckhart C, Philippe TJ, Le François B, Vahid-Ansari F, Geddes SD, Béïque J-C, et al. Sex-dependent adaptive changes in serotonin-1A autoreceptor function and anxiety in Deaf1-deficient mice. Mol. Brain. 2016;9 Available from: https://www.ncbi.nlm.nih.gov/pmc/articles/PMC4973060/

Mainguy G, Ernø H, Montesinos ML, Lesaffre B, Wurst W, Volovitch M, et al. Regulation of epidermal bullous pemphigoid antigen 1 (BPAG1) synthesis by homeoprotein transcription factors. J. Invest. Dermatol. 1999;113(4):643–50

Michelson RJ, Collard MW, Ziemba AJ, Persinger J, Bartholomew B, Huggenvik JI. Nuclear DEAF-1-related (NUDR) protein contains a novel DNA binding domain and represses transcription of the heterogeneous nuclear ribonucleoprotein A2/B1 promoter. J. Biol. Chem. 1999;274(43):30510–9

Philippe TJ, Vahid-Ansari F, Donaldson ZR, Le François B, Zahrai A, Turcotte-Cardin V, et al. Loss of MeCP2 in adult 5-HT neurons induces 5-HT1A autoreceptors, with opposite sex-dependent anxiety and depression phenotypes. Sci. Rep. 2018;8 Available from: https://www.ncbi.nlm.nih.gov/pmc/articles/PMC5893553/

Vulto-van Silfhout AT, Rajamanickam S, Jensik PJ, Vergult S, de Rocker N, Newhall KJ, et al. Mutations affecting the SAND domain of DEAF1 cause intellectual disability with severe speech impairment and behavioral problems. Am. J. Hum. Genet. 2014;94(5):649–61

#### FIGURE LEGENDS

Figure 1. DEAF1 regulates *EN1* expression. (a) Enrichment of DEAF1 upstream of the *EN1* ORF in human GMA24F1A keratinocytes by ChIP-seq with DEAF1 antibody. Alignments of predicted DEAF1 binding sites (grey rectangles) are shown (dots – identical base). (b) ChIP-PCR validation of DEAF1 enrichment. Average enrichment +/-SD of DEAF1 or IgG over the input for each set of primers. HBG1 promoter used as negative control. Arrows: forward (F) and reverse (R) primers. (c, d) Average *EN1* expression +/-SD by quantitative RT-PCR in GMA24F1A keratinocytes (c) transfected with GAPDH (control) or DEAF1 siRNA and (d) transduced to overexpress DEAF1. (e) Average *En1* expression +/-SD in volar hind-limb skin in *wildtype*, *heterozygous* (Deaf1KO/+) and *knockout* (Deaf1KO) mice. Sidak-adjusted *P* values are reported (\*\**P*<0.01, \*\*\**P*<0.001 and \*\*\*\**P*<0.0001).

Figure 2. Deaf1 loss alters skin appendage composition in the mouse volar skin. (a) Representative images of hind-limb epidermal preparations from adult wildtype, Deaf1 knock-out heterozygous (Deaf1KO/+) and homozygous knock-out (Deaf1KO) animals with magnified views of the IFP. Red arrow: hair follicle, black arrow: eccrine gland. Scale bar = 1mm (b, c) The number of eccrine glands (b) and hair follicles (c) in the IFP of each genotype class. (d) The number of hind-limb IFP eccrine glands of Deaf1<sup>fl/fl</sup>;En1<sup>+/+</sup>, Deaf1<sup>+/+</sup>;En1<sup>Cre/+</sup>, Deaf1<sup>fl/+</sup>;En1<sup>Cre/+</sup>, Deaf1<sup>fl/fl</sup>;En1<sup>Cre/+</sup> adult mice. Means for each genotype class are plotted +/-SD. Phenotype values from individual mice used in these analyses are shown (black triangles). Sidak-adjusted P values are reported (\*\*P<0.01; \*\*\*P<0.001 and \*\*\*\*P<0.0001).

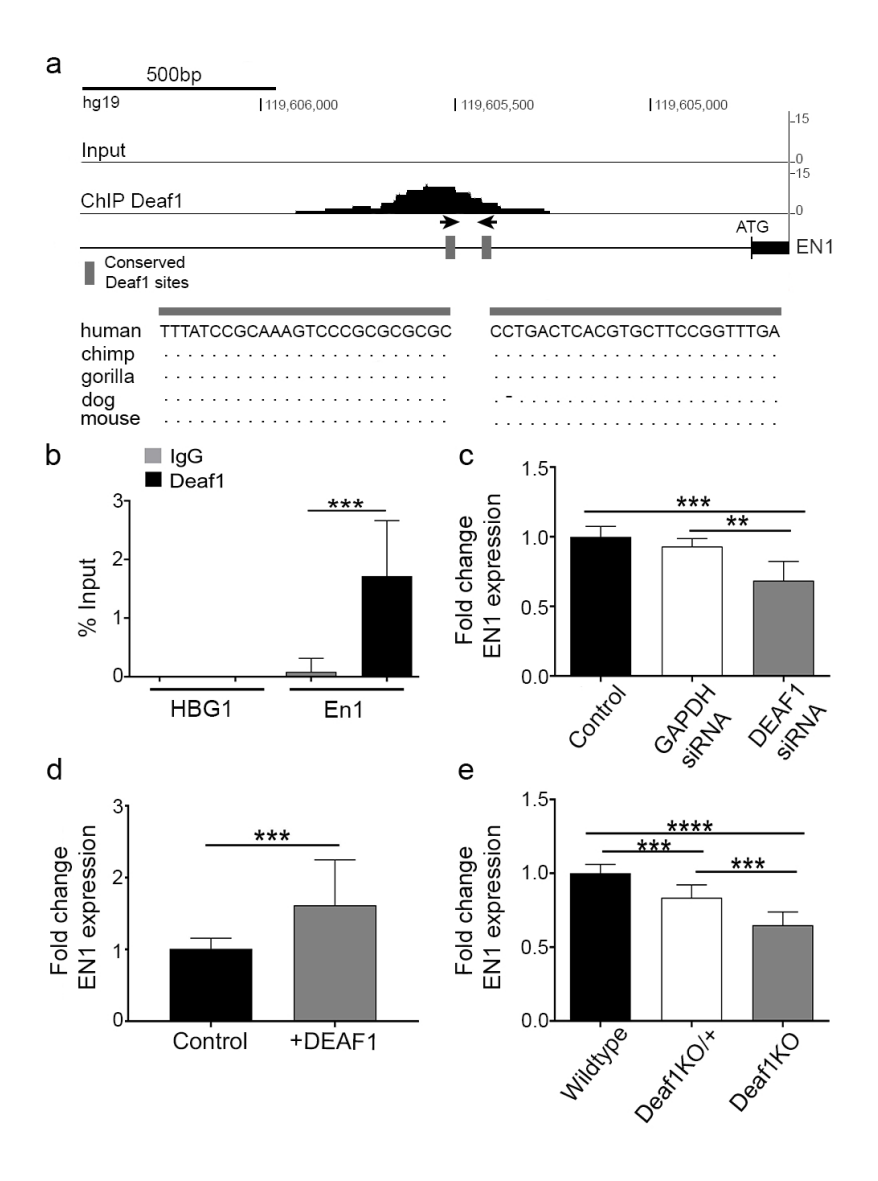


Figure 1. DEAF1 regulates EN1 expression. (a) Enrichment of DEAF1 upstream of the EN1 ORF in human GMA24F1A keratinocytes by ChIP-seq with DEAF1 antibody. Alignments of predicted DEAF1 binding sites (grey rectangles) are shown (dots – identical base). (b) ChIP-PCR validation of DEAF1 enrichment. Average enrichment +/-SD of DEAF1 or IgG over the input for each set of primers. HBG1 promoter used as negative control. Arrows: forward (F) and reverse (R) primers. (c, d) Average EN1 expression +/-SD by quantitative RT-PCR in GMA24F1A keratinocytes (c) transfected with GAPDH (control) or DEAF1 siRNA and (d) transduced to over-express DEAF1. (e) Average En1 expression +/-SD in volar hind-limb skin in wildtype, heterozygous (Deaf1KO/+) and knockout (Deaf1KO) mice. Sidak-adjusted P values are reported (\*\*P<0.01, \*\*\*P<0.001 and \*\*\*\*P<0.0001).

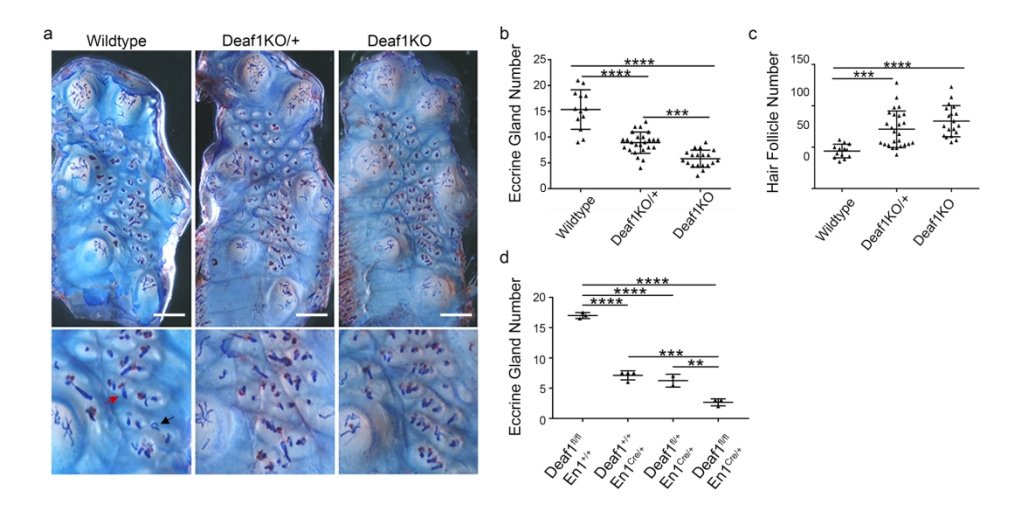


Figure 2. Deaf1 loss alters skin appendage composition in the mouse volar skin. (a) Representative images of hind-limb epidermal preparations from adult wildtype, Deaf1 knock-out heterozygous (Deaf1KO/+) and homozygous knock-out (Deaf1KO) animals with magnified views of the IFP. Red arrow: hair follicle, black arrow: eccrine gland. Scale bar = 1mm (b, c) The number of eccrine glands (b) and hair follicles (c) in the IFP of each genotype class. (d) The number of hind-limb IFP eccrine glands of Deaf1fl/fl;En1+/+, Deaf1+/+;En1Cre/+, Deaf1fl/+;En1Cre/+, Deaf1fl/fl;En1Cre/+ adult mice. Means for each genotype class are plotted +/-SD. Phenotype values from individual mice used in these analyses are shown (black triangles). Sidak-adjusted P values are reported (\*\*P<0.01; \*\*\*P<0.001 and \*\*\*\*P<0.0001).

180x115mm (300 x 300 DPI)

# SUPPLEMENTARY MATERIAL

#### **Materials and Methods**

Mouse strains

Deaf1 knock-out mice were previously generated in the lab of Dr. Stuart Orkin (Dana Farber and Harvard Medical School), and obtained, with permission, from Dr. Paul Albert. Conditional knock-out Deaf1<sup>fl/fl</sup> mice (Vulto-van Silfhout et al. 2014) were obtained from the Mutant Mouse Resource and Research Center and bred to En1<sup>Cre</sup> (Kimmel et al. 2000) to ablate DEAF1 in En1 expressing cells.

Analysis of ectodermal appendage composition

Phenotypic analysis of ectodermal appendage composition in the volar hindlimb skin was carried out as previously described (Kamberov et al. 2013). In brief, three to six week old mice were euthanized and the mouse ventral hindlimb skin was dissected for dissociation in Dispase II (Roche) to isolate epidermal whole mount preparations. Whole mount epidermal preparations were subsequently stained with Nile Blue (Sigma-Aldrich) and Oil Red O (Sigma-Aldrich) to visualize appendages and sebaceous glands, respectively. Eccrine gland ducts and whole hair follicles remained associated with the epidermis. Eccrine gland and hair follicle number was scored by quantifying the number of each appendage type averaged across left and right hindfeet. Representative images were taken on a Leica MZFLIII stereomicroscope equipped with a Nikon DXM1200F camera. Limbs and dissected volar skin for expression analyses were obtained from post-natal day two euthanized animals. All mouse experiments were carried out in accordance with approved Perelman School of Medicine IACUC protocols.

In silico identification of DEAF1 predicted binding sites

DNA binding sites were identified using the Transfac\_2010.1 matrix applied upstream of the *En1* open reading frame (Wingender et al. 2000). Sites conserved across placental mammals were called in this analysis.

# Deaf1 constructs

Full length human DEAF1 was cloned by amplification from a GMA24F1A cDNA library, sequence confirmed and subcloned into pCS4+-HA (gift from Malcolm Whitman Harvard Medical School) or for viral transduction experiments, into pUltra (gift from Malcolm Moore (Addgene plasmid # 24129)) by Gibson assembly. Primers for assembly into pCS4+-HA Forward: TGGGCCGGCCTAAGATCTGGGAGGACTCGGACTCGGCG and Reverse: GGGAGGCTAGCTATCTAGAGGCTCGAGAGGCCTTGTCACACGGTCACCTTCTCCATC Assembly using primers Forward: into pUltra was carried out CAAAAAGCTTGTCGCCACCGATGGGGCCCGGCTACC and Reverse: AGAGGTTGATATCGATAAGCTTGATATCGTTACTTTCACACGGTCACCTTCTCCATC AC.

# Cell culture, transfection and transduction

GMA24F1A cells, a clonal line of human keratinocytes that expresses EN1 was first described by Dr. Howard Green (Harvard Medical School). These cells were obtained from Dr.

Green and maintained as previously described (Mainguy et al. 1999). HEK293T cells were obtained from the laboratory of Dr. Connie Cepko (Harvard Medical School). GMA24F1A cell line was validated for Krt14 and En1 expression during passaging for the duration of experiments.

Transfection of HEK293T cells was carried out using polyethylenimine (Polysciences Inc.). We used a second generation packaging system to generate the lentiviruses used in this study (gift from Connie Cepko Harvard Medical School). All viruses were produced in HEK293T cells according to established protocols. Transduction of GMA24F1A cells was carried out as previously described (McNeal et al. 2015) and cells were harvested 48 hours post infection. Packaging plasmid psPAX2 was a gift from Didier Trono (Addgene plasmid # 12260), envelope plasmid pCL-VSV was a gift from Connie Cepko (Harvard Medical School)

For *DEAF1* knock-down experiments, GMA24F1A cells were transfected with Lipofectamine RNAiMax reagent (Thermo Fisher) according to the manufacturer's protocols using validated ON-TARGET Plus SMART pool siRNA targeting human *DEAF1* (Dharmacon Catalog #L-020808-01-0005) or human *GAPDH* (Dharmacon Catalog #L-004253-00-0005). Cells were harvested 48 hours post transfection and transcript levels analyzed as described below.

# *Quantitative RT-PCR*

RNA was isolated by TRIzol (Thermo Fisher) extraction followed by clean up and on column DNAse treatment using the RNeasy Mini Kit (Qiagen) according to the manufacturer's instructions. cDNA was generated using SuperScript III (Thermo Fisher) and poly-dT priming. Knock-down and overexpression experiments in keratinocytes were conducted in nine biological replicates. Expression of target genes was normalized to human  $\beta$ -ACTIN. N = 6 biological

replicates per condition used for statistical analysis. For detection of expression levels in vivo, a pool of six volar hind-limb skins of a given genotype constituted a single biological replicate in this analysis. N= 9 biological replicates each for wildtype and Deaf1KO/+ classes, and N= 6 biological replicates for Deaf1KO which were used in statistical analysis. Each biological replicate was analyzed by qRT-PCR in technical triplicates, which were averaged to assign a value to the biological replicate. Expression of target genes was normalized to mouse Rpl13a. Primers sequences: hDEAF1 (Vulto-van Silfhout et al. 2014) F: TACGGTGCCGGAACATCAG, hDEAF1 R: CAAACTCGGTGGGACTGTACC, mDeaf1 F: AGAATGAGCTGCCCACAACT, mDeaf1 R: TCAAAGGTCAGTGCTCCAGA, hEN1 (Gesta al. 2006) F: et TTCGGATCGTCCATCCTCC, hEN1 R: GCTCCGTGATGTAGCGGTTT, F: GTGGTCAAGACTGACTCACAGC, mEn1 R: GCTTGTCTTCTCTTCTTCTTT, mRpl13a F: CAGTGCGCCAGAAAATGC, mRpl13a R: GAAGGCATCAACATTTCTGGAA, hbetaACTIN (Croitoru-Lamoury et al. 2011) F: CATGTACGTTGCTATCCAGGC, hbetaACTIN R: CTCCTTAATGTCACGCACGAT, hGAPDH F:TGCACCACCAACTGCTTAGC, hGAPDH R: GGCATGGACTGTGGTCATGAG.

# Chromatin immunoprecipitation, sequencing, analysis and PCR

GMA24F1A cells were cultured in 10 cm dishes and harvested for immunoprecipitation using the EZ-Magma ChIP HiSens kit (EMD Millipore) according to the manufacturer's instructions. Briefly, DNA was cross-linked by adding formaldehyde (1% final concentration) for 10 minutes at room temperature. After cell lysis, the chromatin was sheared using a Covaris M220 sonicator and time optimized to get chromatin fragments between 100bp and 500bp. Immunoprecipitation was carried out using 1/50 Deaf1 Antibody (gift from Paul Albert, (Czesak

et al. 2012)) or lug of normal rabbit IgG antibody (Sigma Aldrich). Input and immune-precipitated samples were purified using a Qiagen PCR purification kit. For ChIP-seq, library construction was done using NEBNext DNA Ultra II DNA library prep kit for Illumina (New England Biolabs). The library was sequenced using Illumina HiSeq 2500 platform (Perelman School of Medicine Next- Generation Sequencing Core). Bioinformatics analysis was done using the Galaxy platform (usegalaxy.org, Afgan et al. 2018). Briefly, the pipeline includes initial QC to remove adaptors (FastQC), then quality reads were mapped to the human reference genome (hg19) using Bowtie2, later MAPQ was used to remove multi-mapping reads and RmDup was used to remove PCR duplicates. Peaks were called using MACS2. ChIP-seq raw data is available from NCBI Gene Expression Omnibus (GSE129965). Quantitative PCR was done using Power SYBR PCR master mix (Thermo Fisher). DEAF1 occupancy at a given region after the immunoprecipitation was determined as the percentage of enrichment over the input using the following equation 100 × 2<sup>Ct(input) - Ct(IP)</sup> and represented as enrichment of DEAF1 or IgG. Primers used for qPCR: EN1 F: ATTTATCCGCAAAGTCCCGCG, R: TTCAAACCGGAAGCACGTGAGTCA, negative HBG1 promoter F: CCAAGGTCATGGATCGAGTT, HBG1 control promoter ACACTGTGACAGCTGGGATG (Cantù et al. 2011). ChIP followed by PCR to validate ChIPseq data was performed three separate times and the means and variation across experiments are reported.

#### Statistical Analysis

Ordinary one-way ANOVA followed by Sidak multiple comparisons test with a single pooled variance was performed on the means for each dataset using GraphPad Prism version 7.00 for Windows, GraphPad Software, La Jolla California USA, www.graphpad.com.

# **Supplementary Figure Legends**

**Figure S1. Validation of DEAF1 enrichment by ChIP-seq at known target regions.** ChIP-seq was performed using the GMA24F1A human keratinocyte cell line. As a validation of our ChIP-seq analysis, DEAF1 ChIP-seq peaks were detected at *DEAF1* (a) and *EIF4G3* (b) loci, (Jensik et al. 2014; Michelson et al. 1999).

Figure S2: Deaf1 loss does not affect eccrine gland number in mouse footpads. The mean number +/-SD of eccrine glands in wildtype, Deaf1KO/+ and Deaf1KO homozygous null mice in the four most proximal hind-limb footpads (FP) 3, 4, 5, and 6 (Kamberov et al. 2013). Individual data points, representing the average of left and right hind-limbs for each analyzed mouse are shown (grey circles and squares). Significance was assessed by ordinary One-way ANOVA. No significant differences in eccrine gland number were found between genotypes in any of the assayed FPs.

Figure S3. Hair follicle number in Deaf1 conditional loss of function mice. The mean number +/-SD of hair follicles in the volar hind-limb IFP was analyzed in Deaf1<sup>fl/fl</sup>;En1<sup>+/+</sup>, Deaf1<sup>fl/+</sup>;En1<sup>Cre/+</sup>, Deaf1<sup>fl/+</sup>;En1<sup>Cre/+</sup>, and Deaf1<sup>fl/fl</sup>;En1<sup>Cre/+</sup> mice. Phenotype values representing the average number of hairs across left and right hind-limbs for each mouse used in these analyses are shown (black triangles). A power calculation, which takes into account the variance in phenotype, indicates there are insufficient animals to assess the null hypothesis of no difference between genotype classes.

#### References

Afgan E, Baker D, Batut B, van den Beek M, Bouvier D, Čech M, et al. The Galaxy platform for accessible, reproducible and collaborative biomedical analyses: 2018 update. Nucleic Acids Res. 2018;46(W1):W537–44

Cantù C, Ierardi R, Alborelli I, Fugazza C, Cassinelli L, Piconese S, et al. Sox6 enhances erythroid differentiation in human erythroid progenitors. Blood. 2011;117(13):3669–79

Croitoru-Lamoury J, Lamoury FMJ, Caristo M, Suzuki K, Walker D, Takikawa O, et al. Interferon-γ regulates the proliferation and differentiation of mesenchymal stem cells via activation of indoleamine 2,3 dioxygenase (IDO). PloS One. 2011;6(2):e14698

Czesak M, Le François B, Millar AM, Deria M, Daigle M, Visvader JE, et al. Increased Serotonin-1A (5-HT1A) Autoreceptor Expression and Reduced Raphe Serotonin Levels in Deformed Epidermal Autoregulatory Factor-1 (Deaf-1) Gene Knock-out Mice. J. Biol. Chem. 2012;287(9):6615–27

Gesta S, Blüher M, Yamamoto Y, Norris AW, Berndt J, Kralisch S, et al. Evidence for a role of developmental genes in the origin of obesity and body fat distribution. Proc. Natl. Acad. Sci. U. S. A. 2006;103(17):6676–81

Jensik PJ, Vargas JD, Reardon SN, Rajamanickam S, Huggenvik JI, Collard MW. DEAF1 binds unmethylated and variably spaced CpG dinucleotide motifs. PloS One. 2014;9(12):e115908

Kamberov YG, Wang S, Tan J, Gerbault P, Wark A, Tan L, et al. Modeling Recent Human Evolution in Mice by Expression of a Selected EDAR Variant. Cell. 2013;152(4):691–702

Kimmel RA, Turnbull DH, Blanquet V, Wurst W, Loomis CA, Joyner AL. Two lineage boundaries coordinate vertebrate apical ectodermal ridge formation. Genes Dev. 2000;14(11):1377–89

Mainguy G, Ernø H, Montesinos ML, Lesaffre B, Wurst W, Volovitch M, et al. Regulation of epidermal bullous pemphigoid antigen 1 (BPAG1) synthesis by homeoprotein transcription factors. J. Invest. Dermatol. 1999;113(4):643–50

McNeal AS, Liu K, Nakhate V, Natale CA, Duperret EK, Capell BC, et al. CDKN2B Loss Promotes Progression from Benign Melanocytic Nevus to Melanoma. Cancer Discov. 2015;5(10):1072–85

Michelson RJ, Collard MW, Ziemba AJ, Persinger J, Bartholomew B, Huggenvik JI. Nuclear DEAF-1-related (NUDR) protein contains a novel DNA binding domain and represses transcription of the heterogeneous nuclear ribonucleoprotein A2/B1 promoter. J. Biol. Chem. 1999;274(43):30510–9

Vulto-van Silfhout AT, Rajamanickam S, Jensik PJ, Vergult S, de Rocker N, Newhall KJ, et al. Mutations affecting the SAND domain of DEAF1 cause intellectual disability with severe speech impairment and behavioral problems. Am. J. Hum. Genet. 2014;94(5):649–61

Wingender E, Chen X, Hehl R, Karas H, Liebich I, Matys V, et al. TRANSFAC: an integrated system for gene expression regulation. Nucleic Acids Res. 2000;28(1):316–9

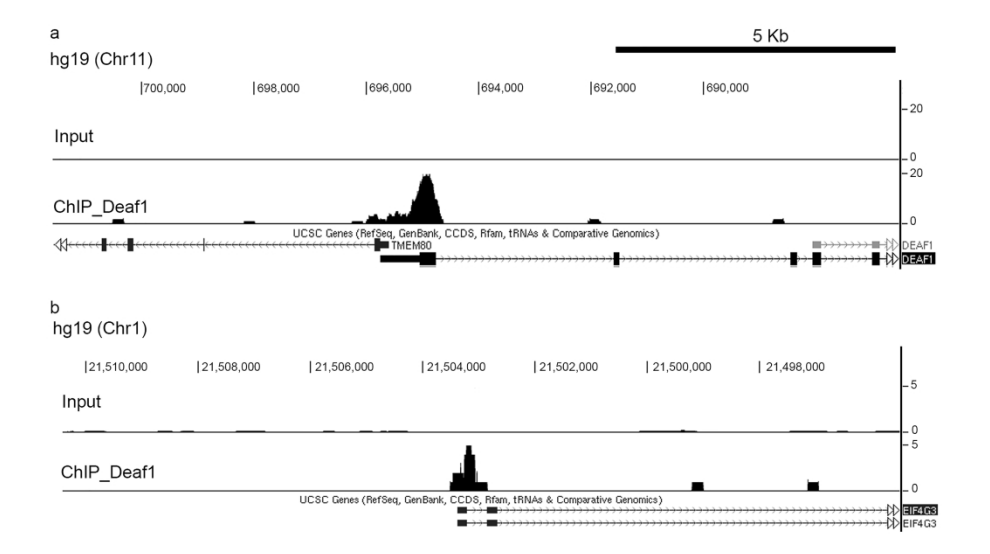


Figure S1. Validation of DEAF1 enrichment by ChIP-seq at known target regions. ChIP-seq was performed using the GMA24F1A human keratinocyte cell line. As a validation of our ChIP-seq analysis, DEAF1 ChIP-seq peaks were detected at DEAF1 (a) and EIF4G3 (b) loci, (Jensik et al. 2014; Michelson et al. 1999).

180x115mm (600 x 600 DPI)

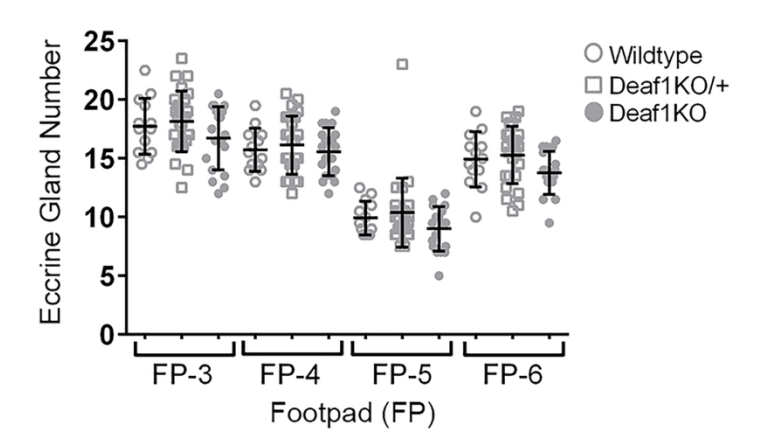


Figure S2: Deaf1 loss does not affect eccrine gland number in mouse footpads. The mean number +/-SD of eccrine glands in wildtype, Deaf1KO/+ and Deaf1KO homozygous null mice in the four most proximal hind-limb footpads (FP) 3, 4, 5, and 6 (Kamberov et al. 2013). Individual data points, representing the average of left and right hind-limbs for each analyzed mouse are shown (grey circles and squares). Significance was assessed by ordinary One-way ANOVA. No significant differences in eccrine gland number were found between genotypes in any of the assayed FPs.

87x49mm (600 x 600 DPI)

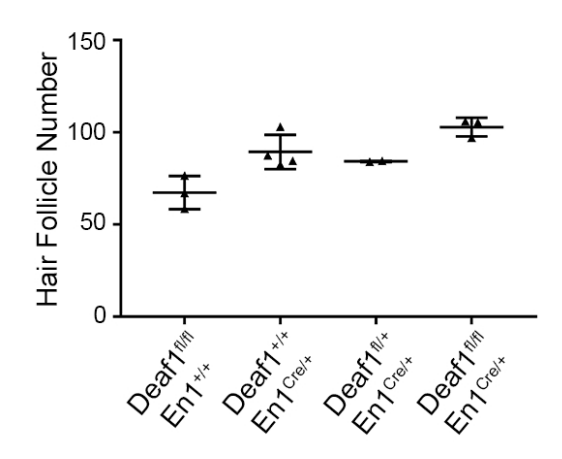


Figure S3. Hair follicle number in Deaf1 conditional loss of function mice. The mean number +/-SD of hair follicles in the volar hind-limb IFP was analyzed in Deaf1fl/fl;En1+/+, Deaf1+/+;En1Cre/+, Deaf1fl/+;En1Cre/+, and Deaf1fl/fl;En1Cre/+ mice. Phenotype values representing the average number of hairs across left and right hind-limbs for each mouse used in these analyses are shown (black triangles). A power calculation, which takes into account the variance in phenotype, indicates there are insufficient animals to assess the null hypothesis of no difference between genotype classes.